Inventory of Supplemental Information, Flynt et al

Figure S1. Repression of yan by miR-1017 is mediated by seed matches
This figure is relevant to main Figure 1. It provides further evidence for the ability of miR-1017 to repress *yan*, specifically via miR-1017 seed matches in its 3' UTR.

Figure S2. Productive expression of mir-1017 variant constructs
This figure is relevant to main Figure 2. It provides further evidence for the productive expression and splicing of variant mir-1017 constructs assayed.

Figure S3. qPCR validation of dsRNA-mediate knockdowns in of S2 cells
This figure is relevant to main Figure 3. It provides evidence for functional knockdown of the intended miRNA/mirtron/exosome pathway targets.

Figure S4. Variable migration of branched mir-1017 precursors that accumulate upon Ldbr knockdown
This figure provides evidence for non-linear mir-1017 precursor molecules.

Figure S5. Processing of a control substrate by recombinant exosome preparations
This figure is relevant to main Figure 3. It provides evidence for activity of all the exosome preps on a control substrate.

Figure S6. Additional 3’ tailed mirtron candidates in D. melanogaster
This figure is relevant to main Figure 4. It depicts loci annotated as candidate 3' tailed mirtrons based on characteristic mapping patterns of small RNA reads to intronic hairpins.

Figure S1. Repression of *yan* by miR-1017 is mediated by seed matches (related to main Figure 1).

The entire 3'UTR of the Ets transcription factor Yan was cloned downstream of renilla luciferase in psiCheck2, which carries a control firefly luciferase gene. The mutant Yan sensor carries specific deletions of the two conserved miR-1017 seed matches (main Figure 1C).

Co-transfection of miR-1017 showed two fold repression of luciferase activity with the construct bearing an intact 3'UTR when compared to the mutant sensor. Luciferase activity was normalized to cells co-transfected with miR-1010 expression construct, a mirtron-derived miRNA that is not predicted to regulate the Yan 3'UTR.
Error bars depict standard deviations.

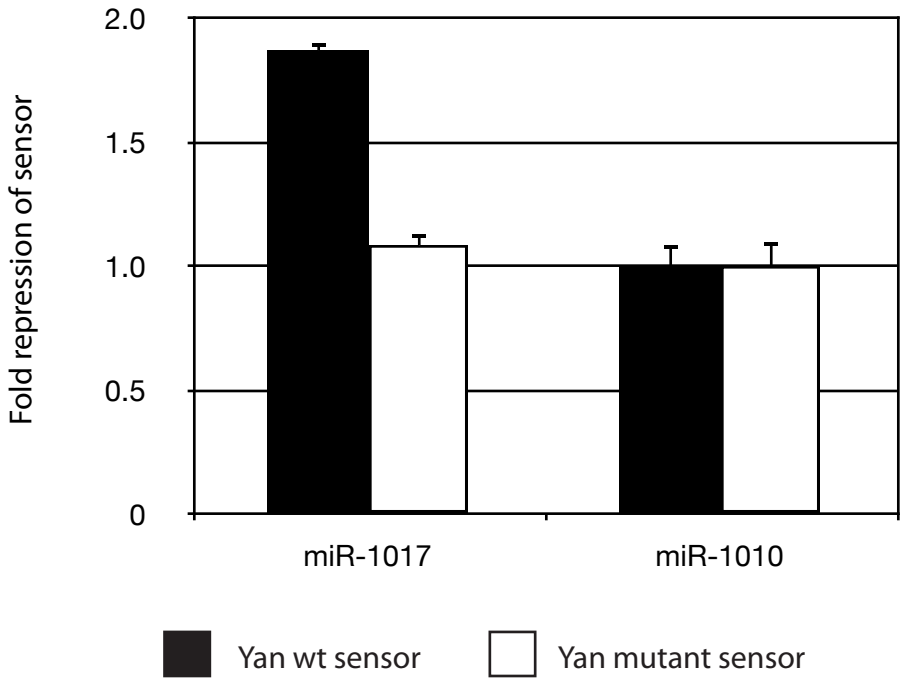

Figure S2. Productive expression of *mir-1017* variant constructs
(related to main Figure 2).

(A) Endogenous fluorescence of cells transfected with *UAS-DsRed-mir-1017* constructs of three Drosophila species--dme, D. melanogaster; dsi, D. simulans, dmo, D. mojavensis--(left), or with a Dme construct mutated in its 5′ splice site or bearing polyG tracts inserted into the intron or exon (right). These cell samples were used in the Northern analysis presented in Figure 2B and 2C. Due to co-transfection of two DsRed plasmids in Figure 2D, fluorescence from pG constructs is from an independent experiment when the mir-1017 poly G construct is tranfected alone. Untransfected control demonstrates no endogenous autofluorescence in the DsRed emission range. (B) Splicing of *mir-1017* polyG (pG) constructs. After reverse transcription PCR is performed with primers located in exonic sequence. Identity of the bands is indicated by the schematic on the left. Splicing products are compared to fragments amplified directly from plamsid DNA. This verifies productive splicing of an tailed mirtron variant that is inefficiently matured into *pre-mir-1017* or mature miR-1017 (Figure 2D).

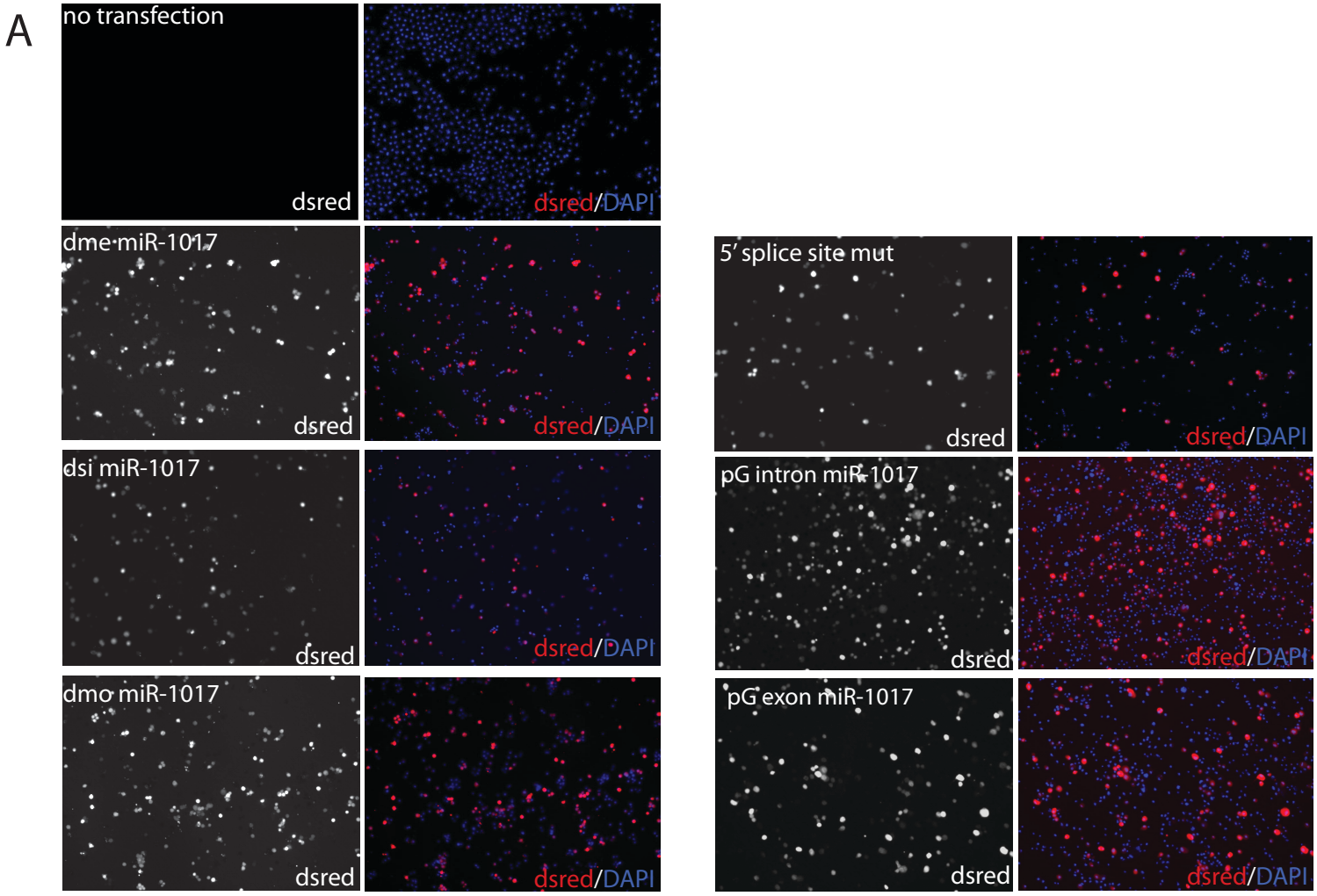

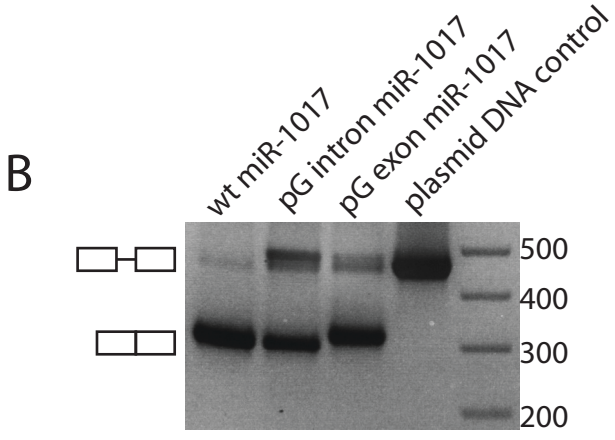

Figure S3. qPCR validation of dsRNA-mediate knockdowns in of S2 cells
(relevant to main Figure 3)

(A) Relative expression of miRNA/mirtron/exosome components after treatment with cognate dsRNA. Knockdown indicated as a percentage of gene expression in GFP dsRNA treated cells; target values were normalized to *Histone 2b* mRNA. Error bars depict standard deviations.

(B) Accumulation of precursor ribosomal RNA following depletion of exosome subunits. Values represent the ratio of pre-rRNA to mature-rRNA, normalized to the ratio in GFP dsRNA treated cells. Error bars depict standard deviations.

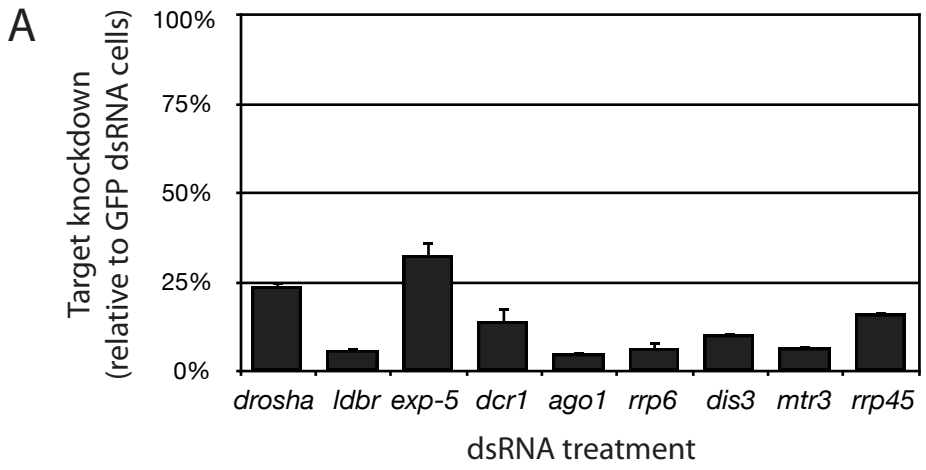

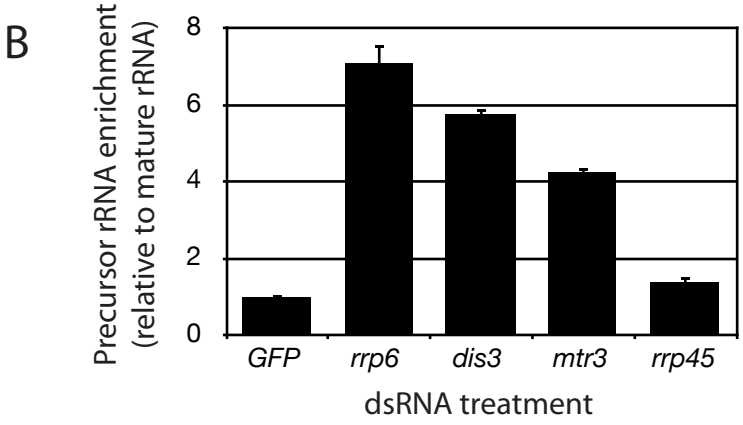

Supplemental Figure 4

Figure S4. Variable migration of branched mir-1017 precursors that accumulate upon Ldbr knockdown

In 16%, 12%, or 8% polyacrylamide gels, mature miR-1017 migrates at ~23-24 nt while the *pre-mir-1017* hairpin migrates at just under 70 nt. Knockdown of lariat debranching enzyme (ldbr) results in loss of hairpin and mature miR-1017. This is accompanied by the accumulation of three bands (indicated by trident) that exhibit highly variable migration in the different percentage gels, indicating non-linear structure. These RNAs likely represent various digested forms of stabilized lariat introns that accumulate upon depletion of Ldbr. The full length (FL)169 nt pri-mir-1017 intron (inferred from its accumulation in exosome knockdowns, main Figure 3B) also exhibited slightly variable migration.

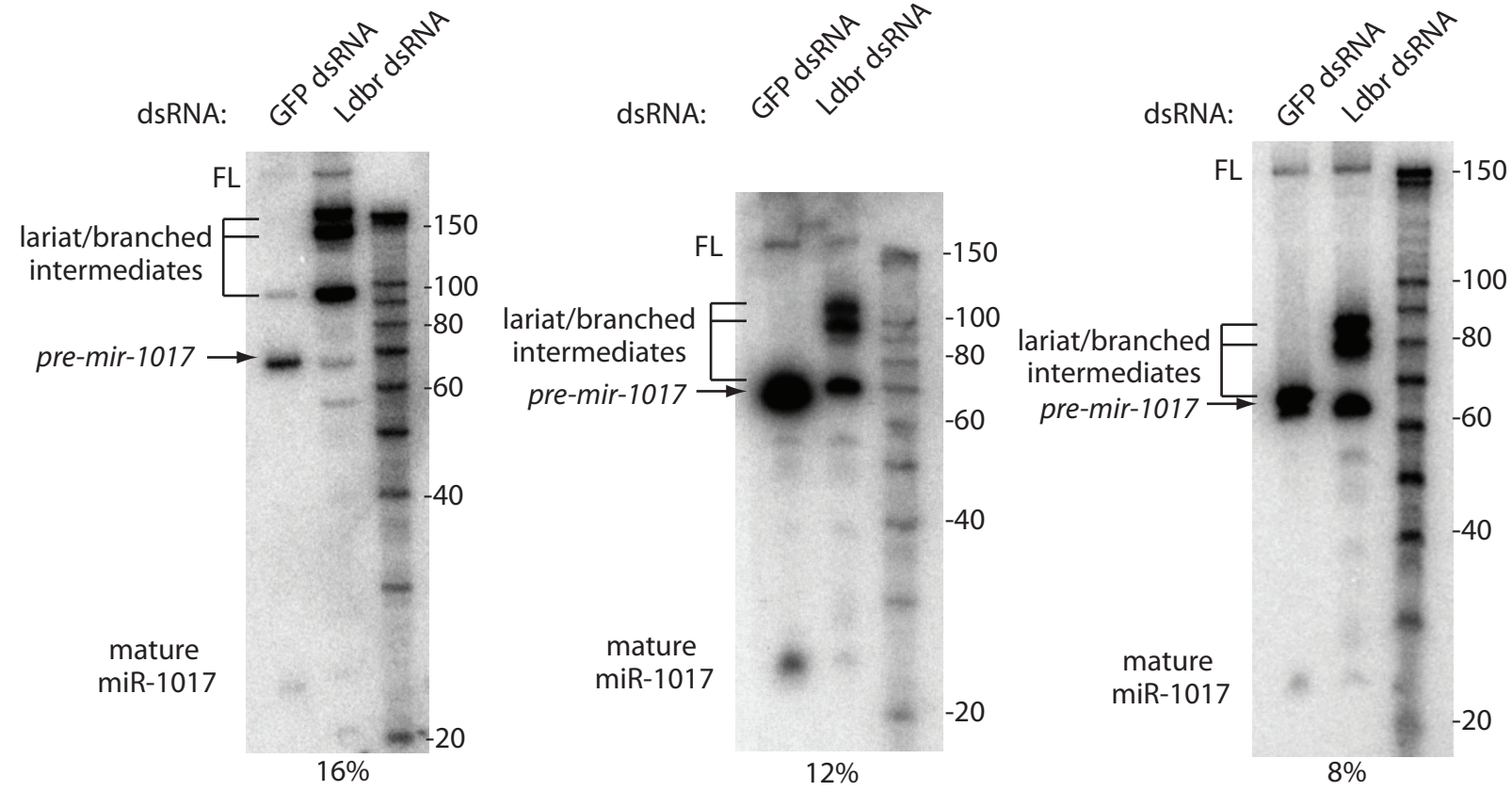

Figure S5. Processing of a control substrate by recombinant exosome preparations (relevant to main Figure 3)

(A) Schematic of RNA substrate. The 5′ end bears a 20nt GNRA tetraloop hairpin, followed by a 29nt unstructured tail.

(B) Incubation of the RNA substrate with aliquots of yExo11, yRrp6, or yExo10, from the same preparations used in main Figure 3E-H, result in efficient degradation of the tail region. Rrp6 was less active on the structured GNRA stem compared to Exo11 or Exo10. Note that these time courses are substantially shorter than those used in main Figure 3 tests of the *pri-mir-1017* intron (20′-160′ incubations). In particular, these data show the yExo10 complex, which was not able to process the *pri-mir-1017* substrate (main Figure 3G), is a functional exonuclease on a different RNA substrate.

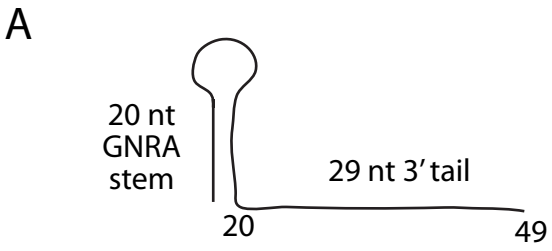

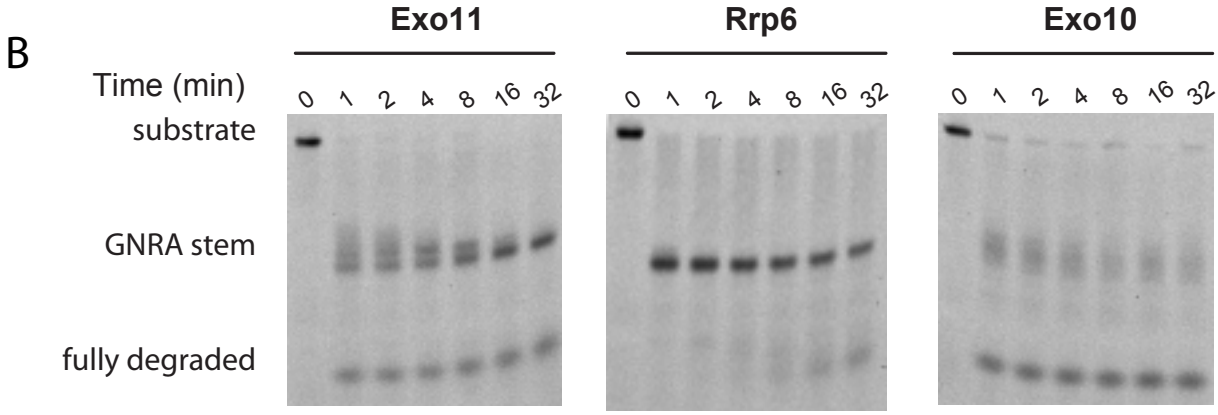

Figure S6. Additional 3′ tailed mirtron candidates in *D. melanogaster*

(relevant to main Figure 4)

Using our previously published small RNA libraries (Chung et al, Current Biology 2008), we searched for intronic hairpins for which only one hairpin end coincided with a splice junction, and that gave rise to cloned small RNAs that were consistent with Dcr-1 cleavage into a miRNA/miRNA* duplex. Although we did not constrain which hairpin end should reside at a splice junction, all six of the loci that fulfilled these criteria were in fact 3' tailed mirtrons, similar to mir-1017. The tails ranged in size from 4-45 nt (highlighted green); *mir-1017* has a ~100 nt tail.
Each locus alignment shows the genomic sequence with flanking exons in lowercase and the intron in uppercase, the predicted secondary structure of the intron in dot-bracket notation, and the short RNA reads recovered. Note that *CG7927_in2/mir-2501* was earlier annotated as the mirtron locus mir-2501 (Berezikov et al, Nature Genetics 2010). In addition, while *mlc-c_in1/mir-3645* is not currently known to be alternatively spliced, the 3p reads of its hairpin end in "AG" or "AGT". We cannot rule out that this might be a conventional mirtron produced by alternative splicing, for which some reads are subject to 3′ uridylation.